Nanoscale

COMMUNICATION

View Article Online
View Journal | View Issue

Cite this: *Nanoscale*, 2016, **8**, 7834

Received 3rd December 2015,
Accepted 13th March 2016

DOI: 10.1039/c5nr08578k

www.rsc.org/nanoscale

Room-temperature Y-type emission of perylenes by encapsulation within single-walled carbon nanotubes†

Masayoshi Tange,* Toshiya Okazaki, Zheng Liu, Kazu Suenaga and Sumio Iijima

Fluorescent materials that exhibit large Stokes shifts are useful for suppressing aggregation-caused quenching. Controlling the self-trapped exciton (STE) states in organic dyes with a dimeric structure is one way of tuning Stokes shifts. However, this leads to the spectral broadening of the emissions at room temperature owing to the effects of the surrounding materials on the excited dimers. Here, we demonstrate the effects of confining organic dyes on their optical properties *via* the encapsulation of perylene molecules within single-walled carbon nanotubes. The encapsulated dimeric perylene exhibits fluorescence with large Stokes shifts and long lifetimes through the STE states. In particular, a noticeable emission of dimeric perylene is observed with a vibronic structure at room temperature; this resembles the Y-type emission of dimeric α-perylene crystals observed only at low temperatures. The results suggest that the isolation of the excited perylene dimers plays an important role in the occurrence of the room-temperature Y-emission.

The Stokes shift of fluorescent materials is an attractive characteristic for solar energy harvesting and biomolecular imaging.[1–3] Large differences between the excitation and emission wavelengths can lead to improvements in the fluorescence quantum yield, the extent of light concentration, and radiation detection sensitivity, because Stokes shifts allow for wavelength conversion and result in low self-absorption. In particular, luminescent species with large Stokes shifts are used widely as materials in luminescent solar concentrators.[4–6]

Organic dye materials with dimeric molecular structures can cause noticeable emissions with large Stokes shifts owing to the presence of self-trapped exciton (STE) states, which are attributable to the coupling between the excitons and phonons in the crystal lattice because the nonlinear interaction leads to exciton localization.[7,8] However, not only does an increase in the temperature lead to the transfer of excitation energy to the surrounding materials, but variations in the intermolecular distance in the dimeric structure can also result in the spectral broadening of the emissions. This is because of the sensitivity of the emission peaks to the molecular arrangement.[9] Therefore, the geometrical confinement of the organic dyes is necessary for controlling their optical properties.[10] The spatial confinement of other components within single-walled carbon nanotubes (SWCNTs) has been employed for a wide range of purposes such as synthesizing hybrid nanostructures, modulating the photophysical and electronic characteristics of SWCNTs, and improving the stability and robustness of the chemical and photophysical properties of the guest components.[11–17] In particular, the individual molecules are isolated on the nanometer scale by the walls of the nanotubes.[18] Hence, the encapsulation of fluorescent molecules within SWCNTs can be expected to prevent aggregation-caused quenching.

The molecular dye perylene is one of the most interesting guest components for the encapsulation of planar π-conjugated compounds. The compound exhibits visible fluorescence, the properties of which depend on its molecular configuration; its emission wavelength, spectral shape, and fluorescence lifetime change dramatically with changes in its molecular arrangement.[7,8,19–22] In particular, perylene dimers and α-perylene, which is a crystal with a dimeric structure, exhibit characteristic emissions from the STE states that lead to large Stokes shifts. Moreover, depending on the temperature, perylene exhibits a Y (Yellow) or E (Excimer) emission; two different STE states (*i.e.*, the Y- and E-states) are responsible for these emissions.[23,24] At temperatures lower than 50 K, the Y-emission, identifiable by a vibronic fine structure, occurs because the Y-state is metastable and there is a potential barrier between the Y- and E-states. In contrast, at higher temperatures, an E-emission with a broad spectral shape

National Institute of Advanced Industrial Science and Technology (AIST), Tsukuba 305-8565, Japan. E-mail: masa-tange@aist.go.jp

†Electronic supplementary information (ESI) available: Experimental details; simulated molecular arrangements of perylenes encapsulated within SWCNTs; optical absorption spectrum of perylene in *n*-hexane; excitation and emission spectra of perylenes@Arc-SWCNTs and the mixture of perylenes and HiPco-SWCNTs in SDBS/D_2O; excitation spectrum of perylenes@HiPco-SWCNTs in SDBS/D_2O; emission spectrum of a concentrated perylene solution; photoluminescence excitation map of perylenes@HiPco-SWCNTs in SDBS/D_2O. See DOI: 10.1039/c5nr08578k

occurs owing to thermal fluctuations, resulting from relaxation from the Y-state to the E-state. Furthermore, the optical properties of perylene, such as its emission spectrum and fluorescence lifetime, are determined by the crystal size and the surrounding molecules.[21,22,25–27]

In this work, to demonstrate the effects of the isolation of a low-dimensional molecular arrangement of an organic dye on the optical properties of its fluorescence emissions, we encapsulated perylene molecules within SWCNTs *via* a vapor-phase doping technique[15,28,29] that involved the sublimation of the guest molecules. We then examined the properties of the encapsulated perylene molecules by optical spectroscopy. We found that the perylene confined within individual SWCNTs exhibited different emission spectra, which varied with the tube diameter (d_t). Specifically, the emissions of the encapsulated dimeric perylene chains exhibited large Stokes shifts but were different from those of perylene dimers and α-perylene at room temperature, suggesting that the phenomenon of geometrical confinement has a significant effect on exciton–phonon coupling in dimeric perylene.

When perylene molecules are encapsulated within SWCNTs, the arrangement of the molecules depends on the diameter of the SWCNTs. High-resolution transmission electron microscopy (HRTEM) images of perylene molecules confined in two types of SWCNTs (small-diameter tubes: HiPco-SWCNTs with d_t = 0.8–1.3 nm and large-diameter tubes: Arc-SWCNTs with d_t = 1.2–1.6 nm) are shown in Fig. 1; the images indicate that the molecular arrangement of the perylene molecules encapsulated within the SWCNTs varies with the value of d_t. Further, the molecular arrangement can be classified into three different types. As shown in Fig. 1a and b, the encapsulated perylene molecules form monomeric and dimeric perylene linear chains along the tube axis in the case of small-diameter tubes with diameters lower than ~1.0 nm and intermediate-diameter tubes with diameters of 1.0–1.3 nm, respectively. On the other hand, in the case of large-diameter tubes with diameters greater than 1.3 nm, the longest axis of the perylene molecules tilts in the radial direction of the SWCNTs, as shown in Fig. 1c. Consequently, the encapsulated perylene molecules form a disordered dimeric structure. The three different types are supported by the molecular arrangements which we simulated to speculate about the encapsulated perylenes (Fig. S1 in the ESI†).

To characterize the fluorescence profile of the encapsulated perylene molecules at room temperature, the emission spectra of perylenes@HiPco-SWCNTs dispersed in D_2O with sodium dodecylbenzene sulfonate (SDBS) were obtained at different excitation wavelengths (380 and 470 nm); the spectra are shown in Fig. 2. In addition, the excitation and emission spectra are shown in the inset to indicate the Stokes shifts. Using the monomer emission shown in Fig. 2 as a reference spectrum, it can be seen that the emission spectrum obtained for an excitation wavelength (λ_{ex}) of 380 nm exhibits two peaks (at approximately 444 and 474 nm) that confirm the presence of the monomeric perylene linear chain shown in Fig. 1a, as well as high-intensity peaks centered at approximately 514 and 548 nm, along with a shoulder at approximately 590 nm. The spectral component in the long-wavelength range has a markedly different shape from that of the spectrum of the perylene monomers. Moreover, when perylenes@HiPco-SWCNTs are excited under visible light with a wavelength of 470 nm, which is longer than the absorption wavelengths of the perylene monomers (340–450 nm),[20,30] the monomer-related emission component disappears from the spectrum. Consequently, perylenes@HiPco-SWCNTs exhibit an emission spectrum with only the two high-intensity peaks and the shoulder; the other prepared solutions of perylene@HiPco-SWCNTs also exhibit

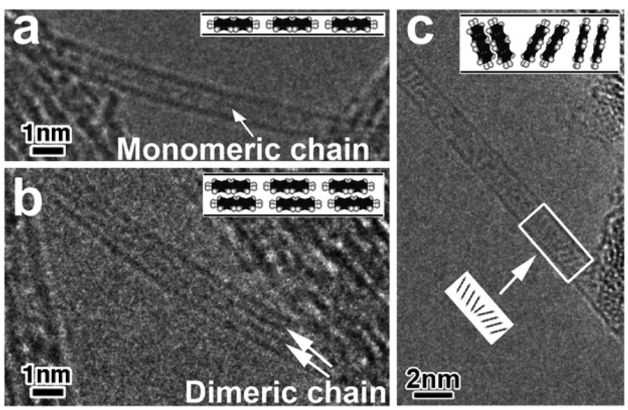

Fig. 1 Typical HRTEM images of (a) a monomeric perylene chain, (b) a dimeric perylene chain, and (c) the disordered dimeric structure corresponding to perylene molecules encapsulated within SWCNTs with different diameters. The insets show the configurations of the perylene molecules. The monomeric and dimeric chains were observed in perylenes@HiPco-SWCNTs; the disordered dimeric structure corresponds to perylenes@Arc-SWCNTs.

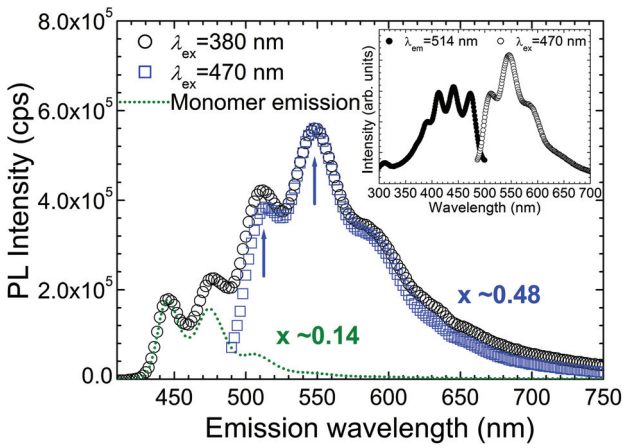

Fig. 2 Emission spectra of perylenes@HiPco-SWCNTs in SDBS/D_2O; the reference spectrum (dotted line) of perylene monomers in SDBS/D_2O (concentration of 8×10^{-5} g L^{-1}) is also shown for comparison. The energy difference between the two peaks marked by arrows is approximately 1200 cm^{-1}. The inset shows the excitation and emission spectra of the perylene molecules confined within SWCNTs, indicating a large Stokes shift of approximately 40 nm for dimeric perylene chains.

this spectral component. The fact that different emission spectra are obtained for different excitation wavelengths indicates that the perylene molecules are arranged in different arrangements in the SWCNTs in the case of perylenes@HiPco-SWCNTs; this is supported by the different morphologies shown in Fig. 1a and b. It is interesting to note that, for visible-light excitations that have lower energies compared to the absorption bands of perylene monomers, the shape of the emission spectrum is determined by vibronic coupling; thus, these emissions are more similar to the Y-emission observed at low temperatures in the case of dimeric α-perylene crystals and perylene dimers than to the E-emission observed at high temperatures. The peak position is consistent with that of the Y-emission of perylene dimers; the perylene dimers are characterized by a large Stokes shift (~45 nm).[21,22] Moreover, normally, in the case of the spectrum of Y-emission, there is a difference of approximately 1100 cm^{-1} between the first two peaks, because these peaks are attributable to one-phonon-assisted transitions associated with two intramolecular vibrational modes;[7,8] the emission spectrum of perylenes@HiPco-SWCNTs also shows such an energy separation (approximately 1200 cm^{-1}), as represented by the two peaks (marked with arrows) in Fig. 2. That the shape of the emissions of the dimeric perylene chains is such, suggests that the Y-state becomes stable at room temperature owing to the isolation of dimeric perylene, which, in turn, is attributable to the encapsulation of perylene by the SWCNTs.

As shown in the inset of Fig. 2, the excitation spectrum of perylenes@HiPco-SWCNTs for an emission wavelength (λ_{em}) of 514 nm also has a shape different from that of the excitation spectrum of the perylene monomers[31] and contains a peak centered at 470 nm. Further, the lowest energy-absorption band of perylenes@HiPco-SWCNTs is significantly lower than the lowest energy-absorption band of the perylene monomers (Fig. S2 in the ESI†).[20,30] This red-shifted excitation peak is probably attributable not to the monomeric perylene structure, but to the dimeric perylene structure, given the absorption and excitation spectra of dimeric α-perylene crystals and perylene dimers.[20,21] Moreover, the Stokes shift of approximately 40 nm is significantly larger than that observed in the case of perylene monomers (a few nanometers); also, the Stokes shift of perylene monomer emissions in the mixture of perylenes and HiPco-SWCNTs dispersed in SDBS/D_2O is about 6 nm (see Fig. S3 in the ESI†). Using the relationship between the polaron binding energy, E_b, and the Stokes shift, S (for example, $E_b = S/2$ for the Y-state),[8] we can surmise from the large Stokes shift that the E_b is 805 cm^{-1}. This value is as large as the 650 cm^{-1} value derived in the case of dimeric α-perylene crystals. As the STE states, which occur in the dimeric molecular structure, are distinguished by large Stokes shifts and long fluorescence lifetimes,[8] the large Stokes shift observed also supports the conclusion that the emission spectrum of perylenes@HiPco-SWCNTs for excitation wavelengths longer than 470 nm is attributable to dimeric perylene chains.

In addition, the fluorescence lifetime suggests that this long-wavelength component in the emissions of perylenes@HiPco-SWCNTs is caused by the STE states. Fig. 3a shows the fluorescence decay curves of the solution of perylenes@HiPco-SWCNTs; the curves were obtained using light sources with excitation wavelengths similar to those used for the emission spectra shown in Fig. 2. For comparison, the fluorescence decay curves of a solution of a mechanical mixture of HiPco-SWCNTs and perylenes are also shown in Fig. 3b, along with its emission spectrum (see the inset). The mechanical mixture has an emission profile whose spectral shape and peak positions are similar to those of the perylene monomers (see Fig. 2). This suggests that the perylene particles in the mechanical mixture, such as the dimeric α- and monomeric β-perylene crystals, were removed during ultracentrifugation of the solution while preparing the sample solution.

According to the multiexponential model for the fluorescence intensity, I, namely, $I(t) = A\exp(-t/\tau_1) + B\exp(-t/\tau_2)$ (where A and B are coefficients representing the relative contri-

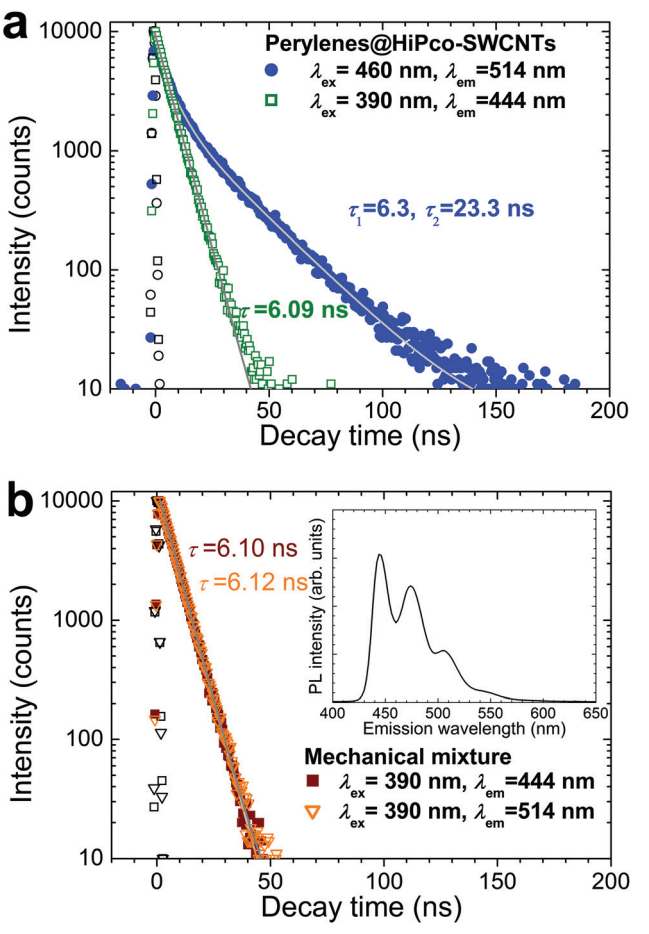

Fig. 3 Fluorescence decay curves of (a) perylenes@HiPco-SWCNTs and (b) a mechanical mixture of HiPco-SWCNTs and perylenes in SDBD/D_2O. The single and multi-exponential decays are plotted along with the estimated lifetimes (τ), which are represented by solid lines to act as visual guides, while the instrument response function for each measurement is represented by the black symbols. The inset shows the emission spectrum of the mechanical mixture when excited at a wavelength of 380 nm.

butions of the two fluorescence components and t and τ are the decay time and fluorescence lifetime, respectively),[32] the fluorescence lifetimes of the short- and long-wavelength components of the emissions of perylenes@HiPco-SWCNTs can be estimated from their fluorescence decay curves. The decay curve for the 444 nm emission obtained using 390 nm excitation radiation exhibits a lifetime of approximately 6 ns. This value is close to those of the emissions of perylene monomers,[33,34] as well as that of the emission of the mechanical mixture (see Fig. 3b), suggesting that the short-wavelength component of the emissions of perylenes@HiPco-SWCNTs is caused by the monomeric structure of perylene. In contrast, the decay curve of the 514 nm emission obtained using 460 nm excitation radiation exhibits not only a short-lifetime component but also a longer-lifetime component with a lifetime of approximately 23 ns; the short fluorescence lifetime (τ_1 = 6.3 ns) appears because the tail of the lowest energy-absorption band for monomer-related emissions is red-shifted (see Fig. S4 in the ESI†). The long fluorescence lifetime of perylenes@HiPco-SWCNTs is comparable to that of the Y-emissions observed at 25 K in α-perylene crystals.[35] The presence of the longer-lifetime component suggests that the long-wavelength component of the emissions includes emissions from the STE states. Moreover, as is the case with the spectral shape of the long-wavelength component, its lifetime is also more similar to that of the Y-emission than that of the E-emission.[7,8,24] Therefore, the emissions of the dimeric perylene chains in perylenes@HiPco-SWCNTs, which have a long lifetime, can be considered as Y-emissions in terms of their spectral shape, which exhibits a vibronic fine structure and a large Stokes shift.

Normally, a system consisting of a mixture of different molecules with spectral overlap between the emission donor band and the absorption acceptor band exhibits a large Stokes shift in terms of energy transfer from the donor molecules to the acceptor molecules.[36] However, the large-Stokes-shifted emissions in the inset of Fig. 2 occurred when perylenes@HiPco-SWCNTs were excited at an energy corresponding to the lowest energy absorption peak (centered at approximately 470 nm), suggesting that the perylenes had a dimeric structure; the excitation energy is lower than the absorption bands for monomer-related emissions (see Fig. S4 in the ESI†). Therefore, this large Stokes shift, which is related to STEs, occurs because of a photophysical process different from the transfer of energy from the donor molecules to the acceptor molecules.

Interestingly, when perylene molecules are encapsulated within larger-diameter SWCNTs, it results in the spectral broadening of the long-wavelength component of their emissions (see Fig. S5 in the ESI†). In perylenes@Arc-SWCNTs, the encapsulated perylene molecules form a disordered dimeric structure, owing to the large diameter of the encapsulating tubes, as shown in Fig. 1c. The resultant variations in the intermolecular distance in the structure can lead to the broadening of the absorption and emission spectra. In fact, perylenes@Arc-SWCNTs exhibit a broader Y-emission with a peak centered at approximately 550 nm when excited at 470 nm (Fig. S5 in the ESI†); owing the disordered molecular configuration, the excitation spectrum also has a broader shape (Fig. S6 in the ESI†) and the broad absorption band is similar to that of perylene aggregates.[37] Moreover, with an increase in the excitation wavelength, the shape of the emission spectrum changes and the peak at 550 nm is suppressed. The shapes of the spectra obtained at the longer-wavelength excitations also are similar to that of the E-emission of perylene aggregates (see also Fig. S7 in the ESI†).[37] This similarity between the E-emission of perylene and the emissions of perylenes@Arc-SWCNTs suggests that the interactions between dimeric perylene and the surrounding environment (adjacent perylene dimers or SWCNTs) are enhanced because of the disordered structure and that this promotes the relaxation of the molecules from the Y-state to the E-state.

Similar to the energy shifts related to the optical transitions due to fullerenes encapsulated within SWCNTs,[28,38,39] whose tube structures were identified by their chiral indices (n, m), perylenes@HiPco-SWCNTs also exhibited tube-structure-dependent energy shifts in the optical transitions of SWCNTs, as determined from the photoluminescence excitation (PLE) map (see Fig. S8 in the ESI†). Moreover, although an investigation of the interaction of the encapsulated perylenes with the different (n, m) species of the SWCNTs will require a detailed spectroscopic analysis of the optical properties of the SWCNTs, in the PLE map of perylene@HiPco-SWCNTs, for example, the (12, 5) SWCNTs did not induce noticeable energy shifts. This suggests that a smaller strain acts on the SWCNTs; the tube diameter of the semiconducting SWCNTs being 1.20 nm allows for the formation of dimeric perylene chains. In addition, the PLE map characterized by the well-resolved PL peaks of the different (n, m) species is different from that of the bundled SWCNTs indicating significant exciton energy transfer,[40] suggesting the transfer of less energy from the small-diameter tubes with the encapsulated monomeric perylene chains to the larger-diameter tubes with the encapsulated dimeric chains.

The effect of confinement on the fluorescence lifetime of the encapsulated molecules will also be dependent on the tube structure, which governs the inner space and the electronic characteristics of the SWCNTs, because of a change in the interaction between the SWCNTs and the encapsulated molecules. In fact, although the variation in the fluorescence lifetime is small, a relatively strong interaction leads to a decrease in the fluorescence lifetime of the encapsulated molecules,[17] whereas a weaker interaction, which results in the isolation of the encapsulated molecules, leads to an increase in the fluorescence lifetime.[41] Therefore, the fluorescence lifetimes for both the Y-emissions of the dimeric perylene chains and the monomer-related emissions of the monomeric perylene chains may also be influenced by the tube structure of the SWCNTs. In order to be able to control the optical properties of dimeric perylene, the perylene molecules should be encapsulated within semiconducting SWCNTs with specific diameters. Semiconducting SWCNTs with the desired characteristics can be prepared using selective-extraction

methods such as the polymer wrapping technique.[42] Therefore, the confinement effects of perylene molecules encapsulated within SWCNTs and the use of selective-extraction techniques to obtain SWCNTs with the desired characteristics should promote the use of encapsulated organic dyes for photovoltaic devices.

Conclusions

We demonstrated the effects of the confinement of organic dyes on their optical properties *via* the encapsulation of perylene molecules within SWCNTs. The arrangement of the encapsulated perylene changes from monomeric linear chains to dimeric linear chains and finally to disordered dimeric structures with an increase in d_t. These changes in the arrangement of perylene lead to changes in the spectral shape, Stokes shift, and lifetime of its emissions. In particular, the encapsulated dimeric perylene not only leads to large Stokes shifts, owing to the formation of STE states, but also exhibits a room-temperature Y-emission with a vibronic fine structure corresponding to the dimeric perylene chains. However, in the case of α-perylene crystals and perylene dimers, the Y-emission occurs only at low temperatures. In addition, the fact that the emissions of disordered dimeric perylene encapsulated in larger-diameter tubes are broader suggests that the Y-emission at room temperature is attributable to the confinement effect. Thus, by exploiting this confinement effect and using selective-extraction techniques to obtain SWCNTs with specific diameters, it would be possible to control the emissions of encapsulated organic dyes with precision.

Acknowledgements

The authors thank Dr. T. Saito (National Institute of Advanced Industrial Science and Technology) for the experimental assistance. M. T. acknowledges support from the Japan Society for the Promotion of Science (grant no. 09J07245, 24760607) and the Hatakeyama Culture Foundation.

Notes and references

1 M. J. Currie, J. K. Mapel, T. D. Heidel, S. Goffri and M. A. Baldo, *Science*, 2008, **321**, 226–228.
2 I. L. Medintz, H. T. Uyeda, E. R. Goldman and H. Mattoussi, *Nat. Mater.*, 2005, **4**, 435–446.
3 X. Peng, F. Song, E. Lu, Y. Wang, W. Zhou, J. Fan and Y. Gao, *J. Am. Chem. Soc.*, 2005, **127**, 4170–4171.
4 M. G. Debije and P. P. C. Verbunt, *Adv. Energy Mater.*, 2012, **2**, 12–35.
5 F. Meinardi, A. Colombo, K. A. Velizhanin, R. Simonutti, M. Lorenzon, L. Beverina, R. Viswanatha, V. I. Klimov and S. Brovelli, *Nat. Photonics*, 2014, **8**, 392–399.
6 O. Moudam, B. C. Rowan, M. Alamiry, P. Richardson, B. S. Richards, A. C. Jones and N. Robertson, *Chem. Commun.*, 2009, 6649–6651.
7 H. Sumi, *Chem. Phys.*, 1989, **130**, 433–449.
8 T.-M. Wu, D. W. Brown and K. Lindenberg, *Phys. Rev. B: Condens. Matter*, 1993, **47**, 10122–10134.
9 J. L. Brédas, J. P. Calbert, D. A. da Silva Filho and J. Cornil, *Proc. Natl. Acad. Sci. U. S. A.*, 2002, **99**, 5804–5809.
10 J. Yu, Y. Cui, H. Xu, Y. Yang, Z. Wang, B. Chen and G. Qian, *Nat. Commun.*, 2013, **4**, 2719.
11 B. W. Smith, M. Monthioux and D. E. Luzzi, *Nature*, 1998, **396**, 323–324.
12 J. Sloan, D. M. Wright, H.-G. Woo, S. Bailey, G. Brown, A. P. E. York, K. S. Coleman, J. L. Hutchison and M. L. H. Green, *Chem. Commun.*, 1999, 699–700.
13 K. Yanagi, K. Iakoubovskii, H. Matsui, H. Matsuzaki, H. Okamoto, Y. Miyata, Y. Maniwa, S. Kazaoui, N. Minami and H. Kataura, *J. Am. Chem. Soc.*, 2007, **129**, 4992–4997.
14 J. Lee, H. Kim, S.-J. Kahng, G. Kim, Y.-W. Son, J. Ihm, H. Kato, Z. W. Wang, T. Okazaki, H. Shinohara and Y. Kuk, *Nature*, 2002, **415**, 1005–1008.
15 T. Takenobu, T. Takano, M. Shiraishi, Y. Murakami, M. Ata, H. Kataura, Y. Achiba and Y. Iwasa, *Nat. Mater.*, 2003, **2**, 683–688.
16 K. Yanagi, Y. Miyata and H. Kataura, *Adv. Mater.*, 2006, **18**, 437–441.
17 M. A. Loi, J. Gao, F. Cordella, P. Blondeau, E. Menna, B. Bártová, C. Hébert, S. Lazar, G. A. Botton, M. Milko and C. Ambrosch-Draxl, *Adv. Mater.*, 2010, **22**, 1635–1639.
18 A. N. Khlobystov, *ACS Nano*, 2011, **5**, 9306–9312.
19 B. Stevens, *Spectrochim. Acta*, 1962, **18**, 430–448.
20 J. Tanaka, *Bull. Chem. Soc. Jpn.*, 1963, **36**, 1237–1249.
21 J. Mahrt, F. Willig, W. Storck, D. Weiss, R. Kietzmann, K. Schwarzburg, B. Tufts and B. Trösken, *J. Phys. Chem.*, 1994, **98**, 1888–1894.
22 J. Ferguson, *J. Chem. Phys.*, 1966, **44**, 2677–2683.
23 H. Auweter, D. Ramer, B. Kunze and H. C. Wolf, *Chem. Phys. Lett.*, 1982, **85**, 325–329.
24 B. Walker, H. Port and H. C. Wolf, *Chem. Phys.*, 1985, **92**, 177–185.
25 H. Ishino, S. Iwai, S. Iwamoto, T. Okumura, T. Nishimoto, S. V. Nair, T. Kobayashi and E. Tokunaga, *Phys. Rev. B: Condens. Matter*, 2011, **84**, 041303(R).
26 H. Oikawa, T. Mitsui, T. Onodera, H. Kasai, H. Nakanishi and T. Sekiguchi, *Jpn. J. Appl. Phys.*, 2003, **42**, L111–L113.
27 T. Onodera, H. Kasai, S. Okada, H. Oikawa, K. Mizuno, M. Fujitsuka, O. Ito and H. Nakanishi, *Opt. Mater.*, 2002, **21**, 595–598.
28 T. Okazaki, S. Okubo, T. Nakanishi, S.-K. Joung, T. Saito, M. Otani, S. Okada, S. Bandow and S. Iijima, *J. Am. Chem. Soc.*, 2008, **130**, 4122–4128.
29 T. Okazaki, Y. Iizumi, S. Okubo, H. Kataura, Z. Liu, K. Suenaga, Y. Tahara, M. Yudasaka, S. Okada and S. Iijima, *Angew. Chem., Int. Ed.*, 2011, **50**, 4853–4857.
30 J. Xu, X. Shen and J. R. Knutson, *J. Phys. Chem. A*, 2003, **107**, 8383–8387.

31 T. Vo-Dinh, R. B. Gammage, A. R. Hawthorne and J. H. Thorngate, *Environ. Sci. Technol.*, 1978, **12**, 1297–1302.
32 M. Sauer, J. Hofkens and J. Enderlein, *Handbook of fluorescence spectroscopy and imaging*, Wiley-VCH Verlag GmbH & Co. KGaA, Weinheim, 2011, ch. 1.
33 N. Mataga, Y. Torihashi and Y. Ota, *Chem. Phys. Lett.*, 1967, **1**, 385–387.
34 Y. S. Liu, P. de Mayo and W. R. Ware, *J. Phys. Chem.*, 1993, **97**, 5987–5994.
35 E. von Freydorf, J. Kinder and M. E. Michel-Beyerle, *Chem. Phys.*, 1978, **27**, 199–209.
36 C. Wu, H. Peng, Y. Jiang and J. McNeill, *J. Phys. Chem. B*, 2006, **110**, 14148–14154.
37 L. Latterini, C. Roscini, B. Carlotti, G. G. Aloisi and F. Elisei, *Phys. Status Solidi A*, 2006, **203**, 1470–1475.
38 S. Okubo, T. Okazaki, N. Kishi, S.-K. Joung, T. Nakanishi, S. Okada and S. Iijima, *J. Phys. Chem. C*, 2009, **113**, 571–575.
39 M. Tange, J. K. Kwon, T. Okazaki and S. Iijima, *Jpn. J. Appl. Phys.*, 2014, **53**, 045101.
40 P. H. Tan, A. G. Rozhin, T. Hasan, P. Hu, V. Scardaci, W. I. Milne and A. C. Ferrari, *Phys. Rev. Lett.*, 2007, **99**, 137402.
41 H. Hirori, K. Matsuda and Y. Kanemitsu, *Phys. Rev. B: Condens. Matter*, 2008, **78**, 113409.
42 A. Nish, J.-Y. Hwang, J. Doig and R. J. Nicholas, *Nat. Nanotechnol.*, 2007, **2**, 640–646; F. Chen, B. Wang, Y. Chen and L.-J. Li, *Nano Lett.*, 2007, **7**, 3013–3017; M. Tange, T. Okazaki and S. Iijima, *J. Am. Chem. Soc.*, 2011, **133**, 11908–11911; M. Tange, T. Okazaki and S. Iijima, *ACS Appl. Mater. Interfaces*, 2012, **4**, 6458–6462.